NeuroImage: Clinical 34 (2022) 103022

Contents lists available at ScienceDirect

NeuroImage: Clinical

journal homepage: www.elsevier.com/locate/ynicl

Advanced diffusion imaging to track progression in Parkinson's disease, multiple system atrophy, and progressive supranuclear palsy

Trina Mitchell [a], Bradley J. Wilkes [a], Derek B. Archer [a,b], Winston T. Chu [a,c], Stephen A. Coombes [a], Song Lai [d], Nikolaus R. McFarland [e], Michael S. Okun [e], Mieniecia L. Black [a], Ellen Herschel [f], Tanya Simuni [g], Cynthia Comella [h], Mitra Afshari [h], Tao Xie [i], Hong Li [j], Todd B. Parrish [k], Ajay S. Kurani [g], Daniel M. Corcos [f], David E. Vaillancourt [a,c,e,*]

[a] Laboratory for Rehabilitation Neuroscience, Department of Applied Physiology and Kinesiology, University of Florida, Gainesville, FL, USA
[b] Department of Neurology, Vanderbilt University Medical Center, Nashville, TN, USA
[c] J. Crayton Pruitt Family Department of Biomedical Engineering, University of Florida, Gainesville, FL, USA
[d] Department of Radiation Oncology & CTSI Human Imaging Core, University of Florida, Gainesville, FL, USA
[e] Department of Neurology and the Norman Fixel Institute for Neurological Diseases, College of Medicine, University of Florida, Gainesville, FL, USA
[f] Department of Physical Therapy and Human Movement Sciences, Northwestern University Feinberg School of Medicine, Chicago, IL, USA
[g] Department of Neurology, Northwestern University Feinberg School of Medicine, Chicago, IL, USA
[h] Department of Neurological Sciences, Rush University Medical Center, Chicago, IL, USA
[i] Department of Neurology, University of Chicago Medicine, Chicago, IL, USA
[j] Department of Public Health Sciences, Medical College of South Carolina, Charleston, SC, USA
[k] Department of Radiology, Northwestern Feinberg School of Medicine, Chicago, IL, USA

ARTICLE INFO

Keywords:
Fixel-based analysis
Free-water
Longitudinal
Neurite Orientation and Density
Parkinsonism

ABSTRACT

Advanced diffusion imaging which accounts for complex tissue properties, such as crossing fibers and extracellular fluid, may detect longitudinal changes in widespread pathology in atypical Parkinsonian syndromes. We implemented fixel-based analysis, Neurite Orientation and Density Imaging (NODDI), and free-water imaging in Parkinson's disease (PD), multiple system atrophy (MSAp), progressive supranuclear palsy (PSP), and controls longitudinally over one year. Further, we used these three advanced diffusion imaging techniques to investigate longitudinal progression-related effects in key white matter tracts and gray matter regions in PD and two common atypical Parkinsonian disorders. Fixel-based analysis and free-water imaging revealed longitudinal declines in a greater number of descending sensorimotor tracts in MSAp and PSP compared to PD. In contrast, only the primary motor descending sensorimotor tract had progressive decline over one year, measured by fiber density (FD), in PD compared to that in controls. PSP was characterized by longitudinal impairment in multiple transcallosal tracts (primary motor, dorsal and ventral premotor, pre-supplementary motor, and supplementary motor area) as measured by FD, whereas there were no transcallosal tracts with longitudinal FD impairment in MSAp and PD. In addition, free-water (FW) and FW-corrected fractional anisotropy (FAt) in gray matter regions showed longitudinal changes over one year in regions that have previously shown cross-sectional impairment in MSAp (putamen) and PSP (substantia nigra, putamen, subthalamic nucleus, red nucleus, and pedunculopontine nucleus). NODDI did not detect any longitudinal white matter tract progression effects and there were few effects in gray matter regions across Parkinsonian disorders. All three imaging methods were associated with change in clinical disease severity across all three Parkinsonian syndromes. These results identify novel extra-nigral and

Abbreviations: FAt, free-water corrected fractional anisotropy; FC, fiber bundle cross-section; FD, fiber density; FDC, fiber-density and cross-section; FW, free-water; log-FC, log transformed fiber cross-section; MDS-UPDRS-III, Part III of Unified Parkinson's Disease Rating Scale; MoCA, Montreal Cognitive Assessment; MSAp, parkinsonian variant of multiple system atrophy; NODDI, Neurite Orientation and Density Imaging; ODI, orientation dispersion index; PD, Parkinson's disease; PSP, progressive supranuclear palsy; PSPRS, Progressive Supranuclear Palsy Rating Scale; SMATT, sensorimotor area tract template; TCATT, transcallosal tractography template; UMSARS, The Unified Multiple Systems Atrophy Rating Scale; Vic, intracellular volume fraction; Viso, isotropic volume fraction.

* Corresponding author at: University of Florida, Laboratory for Rehabilitation Neuroscience, Department of Applied Physiology and Kinesiology, PO Box 118205, Gainesville, FL 32611-8205, USA.
E-mail address: vcourt@ufl.edu (D.E. Vaillancourt).

https://doi.org/10.1016/j.nicl.2022.103022
Received 24 January 2022; Received in revised form 29 March 2022; Accepted 24 April 2022
Available online 26 April 2022

extra-striatal longitudinal progression effects in atypical Parkinsonian disorders through the application of multiple diffusion methods that are related to clinical disease progression. Moreover, the findings suggest that fixel-based analysis and free-water imaging are both particularly sensitive to these longitudinal changes in atypical Parkinsonian disorders.

1. Introduction

Parkinson's disease (PD), multiple system atrophy (MSAp), and progressive supranuclear palsy (PSP) are difficult to differentiate clinically especially in the early stages of the disease. This difficulty is thought to be due to overlapping motor symptoms, however, atypical Parkinsonian disorders have differing underlying pathologies and progress devastatingly fast, with symptoms often not responding to current available treatments. Further, all three of these Parkinsonian disorders have nigrostriatal degeneration, (Dickson, 2012) however, MSAp and PSP have widespread pathologies characterized by distinct white and gray matter neurodegeneration throughout the basal ganglia, midbrain, thalamus, cerebellum, corpus callosum, and sensorimotor cortical regions (Ahmed et al., Feb 2008; Cykowski et al., Aug 2015; Wenning et al., Mar 1997; Halliday et al., Oct 2005). In line with this, previous work using advanced diffusion imaging has revealed that cross-sectionally there is increased extracellular fluid in the substantia nigra in PD compared with controls, and also that nigral free-water increases longitudinally over time in *de novo* and early-stage PD (Planetta et al., Feb 2016; Mitchell et al., 2019; Burciu et al., 2017; Ofori et al., 2017). Further, this finding was the only difference detected between PD and controls using free-water imaging and NODDI, two multi-compartmental diffusion imaging methods (Planetta et al., Feb 2016; Mitchell et al., 2019). In comparison, these two advanced multi-compartmental diffusion imaging methods detected distinct differences throughout the basal ganglia, midbrain, cerebellum, and corpus collosum when applied cross-sectionally in both MSAp and PSP when compared to controls (Planetta et al., Feb 2016; Mitchell et al., 2019). Moreover, current literature suggests that extra-nigral and extra-striatal brain regions are important to differentiate MSAp and PSP and may also be important to track longitudinal progression in these atypical Parkinsonian syndromes. Further, biomarkers for tracking disease progression over a relatively short period of time in Parkinsonian disorders are urgently needed to improve clinical trial methodologies and outcomes. While advanced diffusion imaging techniques that account for complex tissue properties are promising for better understanding the disease-specific neurodegeneration that occurs over time in atypical Parkinsonian syndromes, there are very few studies in PD and especially atypical Parkinsonian disorders that have applied these advanced methods longitudinally. This current multi-site cohort study is the first to longitudinally study PD, MSAp, and PSP using three of the most recognized advanced diffusion imaging methods.

Fixel-based analysis is a novel diffusion MRI technique that combines voxel-based analysis with tract-based analysis to address the problem of crossing fibers within a voxel, which can result in misleading outcomes in voxels with a high number of crossing fibers (Raffelt et al., 2017). Fixel-based analysis computes microscopic fiber density (FD) and macroscopic fiber bundle morphology as fiber bundle cross-section (FC), and a combined metric of FD and FC (FDC) (Raffelt et al., 2017; Raffelt et al., 2012). This method has yet to be studied widely because it requires high b-values (e.g., 3000 s/mm^2) which are uncommon in typical diffusion imaging (Raffelt et al., 2017; Raffelt et al., 2012). Cross-sectional studies of PD applying fixel-based analysis have shown altered FD in the corpus callosum and corticospinal tract compared to control subjects (Li et al., 2020). Longitudinal studies of PD applying fixel-based analysis have revealed longitudinal reduction in FDC in the corpus callosum, however, there was not a healthy control group followed to determine if the observations were beyond that of normal aging (Rau et al., 2019). In atypical Parkinsonian syndromes, cross-sectional fixel-based analysis revealed more descending sensorimotor tract involvement in MSAp and PSP compared with PD, and that there was greater corpus callosum impairment in PSP (Nguyen et al., 2021). Furthermore, fixel-based analysis has yet to be applied longitudinally in atypical Parkinsonian disorders and we hypothesize that this technique could capture the wide-spread pathology and longitudinal white matter changes with high sensitivity.

NODDI is a multi-compartment diffusion MRI technique that probes the microstructure of neurites (i.e., axons and dendrites) by modeling three-compartments of the brain tissue (Zhang et al., 2012). This analysis requires a multi-shell diffusion scan with multiple b-values (Zhang et al., 2012). The three compartments modeled are intracellular, extracellular, and CSF. Isotropic volume fraction (Viso) represents the volume fraction of CSF, intracellular volume fraction (Vic) represents the volume fraction of the space bounded by neurites, and orientation dispersion index (ODI) quantifies the degree of dispersion of the neurites. Thus, the two intracellular compartment metrics (ODI, Vic) are corrected for the effect of extracellular fluid. NODDI has been applied cross-sectionally and shown to differentiate the atypical Parkinsonian disorders, MSAp and PSP, from PD (Mitchell et al., 2019). Further, all Parkinsonian syndromes show increased Viso in the substantia nigra compared with controls, whereas MSAp and PSP had widespread involvement of the basal ganglia, midbrain, cerebellum, and corpus callosum cross-sectionally (Mitchell et al., 2019). Select regions that were specific to MSAp were decreased ODI in the putamen and decreased Vic in the middle cerebellar peduncle (Zhang et al., 2012). Regions that were specific to PSP were increased ODI in the superior cerebellar peduncle and decreased ODI in the subthalamic nucleus and pedunculopontine nucleus. Here, changes in ODI could reflect several mechanisms impacting neurites including axonal disorganization, gliosis, dendritic thinning, and other factors (Zhang et al., 2012; Nazeri et al., 2015). NODDI has not been applied longitudinally to atypical Parkinsonian disorders.

Free-water imaging is a two-compartment diffusion imaging technique that has been applied to track progression in PD in the substantia nigra over one year, (Burciu et al., 2017; Ofori et al., 2015) and to distinguish PD from atypical Parkinsonian disorders (Planetta et al., Feb 2016; Mitchell et al., 2019). In FW imaging, tissue is modeled as containing an extracellular compartment and an intracellular tissue compartment, producing two metrics: FW and FW-corrected fractional anisotropy (FAt). FW is the volume fraction of the extracellular compartment and FAt is the fractional anisotropy of the intracellular compartment. Compared to traditional FA, FAt is corrected for the confounding effects of FW (Pasternak et al., Sep 2009). Free-water imaging models an extracellular compartment (i.e., free-water [FW]), and an intracellular tissue compartment (i.e., free-water corrected fractional anisotropy [FAt]) (Pasternak et al., Sep 2009). The advantage behind this type of image post-processing is that it is derived from conventional single-shell diffusion imaging scans. Cross-sectionally, all Parkinsonian syndromes have increased FW in the substantia nigra compared with controls, whereas MSAp and PSP had changes in FW and FAt throughout the basal ganglia, midbrain, cerebellum, and corpus callosum (Planetta et al., Feb 2016; Mitchell et al., 2019). Increased FAt in the putamen was shown to differentiate MSAp, whereas decreased FAt in the superior cerebellar peduncle and increased FAt in the subthalamic nucleus and pedunculopontine nucleus was shown to differentiate PSP (Planetta et al., Feb 2016; Mitchell et al., 2019). Here, reduced FAt in white matter indicates axonal disorganization and degeneration, and increased FAt in gray matter can indicate gliosis or a loss of cell bodies that is related to a

reduction in the isotropy of diffusion (Pasternak et al., Sep 2009; Budde et al., Aug 2011). Free-water imaging has not yet been studied longitudinally in atypical Parkinsonian disorders.

The advanced diffusion imaging modalities implemented here have previously detected cross-sectional impairment in atypical Parkinsonian syndromes and have been suggested to offer promising avenues to detect widespread extra-nigral and extra-striatal pathological changes that occur longitudinally in atypical Parkinsonian disorders. Collectively the modalities better account for complex tissue properties such as crossing fibers in the case of fixel-based analysis, (Raffelt et al., 2017) and extracellular fluid in the case of NODDI and free-water imaging (Zhang et al., 2012; Pasternak et al., Sep 2009). We therefore study these three modalities in tracking longitudinal progression of microstructural changes across white matter tracts and gray matter regions in PD, MSAp, and PSP over a 1-year follow-up.

2. Material and methods

2.1. Participants

37 participants with PD, 17 with PSP, 11 with MSAp, and 21 age- and sex-matched healthy controls completed baseline and 1-year assessments (Table 1). Participants were referred and diagnosed by movement disorder neurologists at the University of Florida, Northwestern University, Rush University, and University of Chicago, based on current diagnostic criteria for PD, MSAp, and PSP (Hoglinger et al., Jun 2017; Gilman et al., 2008; Hughes et al., Mar 1992). The PSP group included 14 PSP patients with the Richardson Syndrome sub-type and three with PSP Parkinsonian variant sub-type. Clinical PSP subtype was determined using established criteria (Hoglinger et al., Jun 2017). Patients were followed and their diagnoses were confirmed as clinically probable at least 2 years after initial diagnosis. Healthy controls were free from neurological disease and had no family history of Parkinsonian disorders. All procedures were approved by the Institutional Review Board at all sites, and written informed consent was obtained from all subjects in accordance with the Declaration of Helsinki.

There was loss to follow-up across all groups, however, it was higher in the atypical Parkinsonian disorder groups. This was impacted largely by rapid disease progression and mortality rates in the MSAp and PSP groups combined with scheduling restrictions related to the covid-19 pandemic. The attrition rates were as follows: the attrition rate in controls was 12.5% (baseline n = 24), in PD was 14% (baseline n = 43), in MSAp was 52.2% (baseline n = 23), and in PSP was 39.3% (baseline n = 28). Only patients with complete baseline and 1-year data are presented in the analyses.

Table 1
Patient Demographics at Baseline.

	Control	PD	MSAp	PSP
N	21	37	11	17
Site 1/2	11/10	17/20	4/7	10/7
Age, years	68.2 (4.8)	65.4 (7.8)	64.77 (7.52)	68.8 (4.8)
Sex, M/F	10/11	20/17	9/2	8/9
Disease Duration, years	–	4.5 (2.8)	3.1 (3.3)	2.8 (2.7)
Hoehn and Yahr stage (I/II/III/IV/V)	–	8/29/1/0/0	0/5/1/2/4	0/6/2/7/2
MDS-UPDRS III, total	4.6 (2.4)	29.4 (13.4)	61.4 (23.6)	43.2 (12.4)
UPDRS posture & gait	0.5 (0.8)	2.0 (1.3)	9.9 (6.5)	9.2 (3.9)
UPDRS rigidity	1.0 (1.3)	5.6 (3.3)	12.2 (4.8)	5.2 (4.2)
UPDRS bradykinesia	2.5 (1.5)	13.0 (7.5)	27.3 (7.7)	22.2 (6.5)
UPDRS tremor	0.6 (1.1)	7.9 (5.5)	8.4 (5.6)	2.2 (1.9)
UMSARS, parts I and II	2.3 (1.9)	17.1 (5.8)	46.0 (16.1)	41.9 (13.3)
PSPRS, total	2.5 (1.8	11.7 (4.5)	34.1 (14.9)	34.8 (12.0)
MoCA	27.3 (2.0)	27.4 (2.6)	25.4 (4.1)	24.1 (3.3)

All variables are presented as mean (standard deviation) except sex and Hoehn and Yahr which are represented as proportions.

All clinical and imaging assessments, administered at baseline and 1-year follow-up, were carried out at the University of Florida and Northwestern University. All participants underwent overnight withdrawal from any dopaminergic medication prior to baseline and follow-up clinical assessments. Overnight withdrawal was done to focus on clinical disease progression to minimize impact of medication changes over 1 year. Motor impairment was assessed using Part III of the Unified Parkinson's disease Rating Scale (MDS-UPDRS-III) (Goetz et al., 2007). Sub-scores for posture and gait (items 9–13), rigidity (item 3), bradykinesia (items 4–8, 13), and tremor (items 15–18) were derived from the MDS-UPDRS-III. The Unified Multiple Systems Atrophy Rating Scale (UMSARS) and the Progressive Supranuclear Palsy Rating Scale (PSPRS) were also used to assess MSAp and PSP specific disease severity (Wenning et al., 2004; Golbe and Ohman-Strickland, Jun 2007). Cognitive function was assessed with the Montreal Cognitive Assessment (MoCA) (Nasreddine et al., 2005). Disease duration was defined as the time since the current diagnosis.

2.2. Imaging and diffusion data acquisition

Data was acquired at the University of Florida McKnight Brain Institute (3 T Siemens Prisma) and Northwestern University Center for Translational Imaging (3 T Siemens Prisma Fit) using a 64-channel head coil. Identical software and pulse sequences were used at each site and quality assurance data published previously indicated signal integrity was stable across sites (Mitchell et al., 2019). T1-weighted images (repetition time: 2000 ms, echo time: 2.99 ms, flip angle: 8°, TI = 1010 ms, GRAPPA factor = 2, 0.8 mm isotropic voxels, bandwidth: 240 Hz/pixel) were acquired with a three-dimensional (3D) magnetization-prepared 180°radio-frequency pulses and rapid gradient-echo (MP-RAGE) sequence in 208 contiguous sagittal slices. Multi-shell diffusion MRI images (repetition time: 3200 ms, echo time: 70 ms, flip angle: 90°, field of view: 256 × 256 mm, resolution: 2 mm isotropic, 64 diffusion gradient directions, b-values: 5 × 0, 64 × 1000, 64 × 2000, and 64 × 3000 s/mm^2, 69 axial slices, bandwidth: 2442 Hz/pixel, total acquisition time: 10 min 52 s) were acquired for fixel-based analysis and NODDI using a simultaneous multi-slice acquisition (acceleration factor = 3). Single-shell diffusion MRI images (repetition time: 6400 ms, echo time: 58 ms, flip angle: 90°, field of view: 256 × 256 mm, resolution: 2 mm isotropic, 64 diffusion gradient directions, b-values: 5 × 0, and 64 × 1000 s/mm^2, 69 axial slices, bandwidth: 2442 Hz/pixel, total acquisition time: 7 min 41 s) were acquired for free-water imaging. One PSP patient was only included in the free-water imaging analysis since there was a data transfer error for the multi-shell acquisition data.

2.3. Diffusion data processing

Fixel-based analysis was performed using MRtrix3 software (Raffelt et al., 2017). Diffusion data were denoised and corrected for susceptibility and motion artifacts (Smith et al., 2004; Andersson and Sotiropoulos, 2016; Veraart et al., 2016). Fiber orientation distribution (FOD) was estimated using multi-shell multi-tissue constrained spherical deconvolution (Jeurissen et al., Dec 2014). Bias field correction and intensity normalization were then performed globally across all subjects (Raffelt et al., 2017). Next, study-specific group-averaged FOD template was created from baseline data, (Rau et al., 2019; Zarkali et al., 2021; Zarkali et al., Feb 2022) and each individual FOD image was warped to this study-specific template using a diffeomorphic non-linear transformation (Raffelt et al., 2011). Apparent FD maps were computed through segmenting each fixel of the FOD images and log transformed fiber cross-section (log-FC) maps were calculated from the distortion required when warping the FOD image to the template (Raffelt et al.,

2017; Raffelt et al., 2012). A combined measure that factors the effects of both fiber density and cross-section (FDC) was also calculated.

NODDI and free-water data processing were performed identically to the previously published cross-sectional part of this study (Mitchell et al., 2019). NODDI maps (Viso, Vic, and ODI) were derived from the pre-processed motion and eddy-current corrected volumes using the NODDI toolbox in MATLAB (Zhang et al., 2012). FW and FAt maps were computed using custom-written MATLAB (R2013a, The Mathworks, Natick, MA, USA) code, as described in previous work (Burciu et al., 2017; Pasternak et al., Sep 2009; Ofori et al., 2015; Archer et al., 2018; Archer et al., Sep 2019). NODDI (Viso, Vic, and ODI) and free-water (FW and FAt) maps were non-linearly transformed into standard MNI space using the Advanced Normalization Tools (ANTs) and in-house templates (Archer et al., 2018; Avants et al., Feb 2008).

White matter tracts were applied to all three diffusion imaging methods. Seventeen white matter tracts from the transcallosal tractography template (TCATT), (Archer et al., 2019) sensorimotor area tract template (SMATT), (Archer et al., 2018) the cerebellar probabilistic white matter atlas, (van Baarsen et al., 2016) and subthalamo-pallidal, nigrostriatal, and corticostriatal tracts (Archer et al., Sep 2019) were used in a tract-of-interest analysis based on their implication in Parkinsonism. Six frontal area tracts were used from the TCATT, the primary motor cortex, dorsal premotor cortex, ventral premotor cortex, supplemental motor area, pre-supplemental motor area, and somatosensory cortex (Archer et al., 2019). The SMATT includes descending sensorimotor tracts from these same six frontal cortical regions (Archer et al., 2018). The superior and middle cerebellar peduncle tracts from the cerebellar atlas were included (van Baarsen et al., 2016). For the fixel-based analysis the MNI-space tracts of interest were non-linearly transformed to the study-specific population template space by applying a warp obtained from registering the FMRIB FA template to the study-specific population FA template (Smith et al., 2004).

We also examined thirteen gray matter regions from the Parkinson's disease region of interest template validated in previous work by our group (Archer et al., Sep 2019). These gray matter regions were used for NODDI and free-water imaging, and not used for fixel-based analysis since this method is focused on white matter. The gray matter regions included: anterior substantia nigra, posterior substantia nigra, putamen, caudate nucleus, globus pallidus, subthalamic nucleus, red nucleus, thalamus, pedunculopontine nucleus, dentate nucleus, cerebellar lobule V, cerebellar lobule VI, and cerebellar vermis (Archer et al., Sep 2019). All white-matter tracts and gray-matter regions were used to obtain mean diffusion measures bilaterally (Planetta et al., Feb 2016; Archer et al., Sep 2019).

2.4. Statistical analyses

All statistical analyses were performed in IBM SPSS version 21.0. Longitudinal change for clinical variables was assessed for each group using paired t-tests or Wilcoxon Signed rank tests in the case of non-parametric variables as determined by a significant Levene's test. Group differences in the 1-year change in clinical variables was assessed using one-way analysis of variance (ANOVA) or Welch's ANOVA for non-parametric variables.

The mean change from baseline to 1-year in fixel-based (FD, log-FC, FDC), NODDI (Viso, ODI, Vic) and free-water (FW, and FAt) maps within each white matter tract was compared between groups using a multivariate ANOVA, with sex, age, site, and baseline value as covariates. The same MANCOVA model was used to assess mean change in the gray matter region-of-interest analysis for NODDI and free-water maps. Significant group effects were corrected for multiple comparisons using the False Discovery Rate (FDR) method ($P_{FDR} < 0.05$) and followed by FDR-corrected pairwise comparisons ($P_{FDR} < 0.05$), performed separately for each diffusion imaging variable. Multiple linear regression was used to determine the association of 1-year change in diffusion measures with clinical disease progression. The regions for fixel-based, free-water, and NODDI with significant change were entered into a backwards stepwise multiple linear regression to predict 1-year change in MDS-UPDRS-III and MDS-UPDRS-III bradykinesia sub-score across Parkinsonism groups.

2.5. Data availability

The data in this study are openly available in the Parkinson's disease biomarker program (https://pdbp.ninds.nih.gov).

3. Results

3.1. Participants and clinical assessments

The interval between baseline and 1-year assessments was 373 days for controls, 376 days for PD, was 376 for MSAp, and 378 for PSP. There was no difference in age ($F_{3,82} = 1.714$, $P = 0.251$), sex distribution ($\chi^2_{3,82} = 4.095$, $P = 0.251$), or disease duration ($F_{2,62} = 2.696$, $P = 0.075$) between groups at baseline (Table 1). PD patients had a longitudinal increase in Hoehn and Yahr stage ($z_{36} = -2.673$, $P < 0.01$), MDS-UPDRS-III total score ($z_{36} = -2.536$, $P < 0.05$), and the posture and gait sub-score ($z_{36} = -3.302$, $P < 0.01$) over one year (Supplemental Table 1). In MSAp, there was an increase in MDS-UPDRS-III total score ($z_{36} = -2.092$, $P < 0.05$) and posture and gait sub-score ($z_{36} = -2.043$, $P < 0.05$) over one year. In PSP, there was a longitudinal increase in Hoehn and Yahr stage ($z_{16} = -3.134$, $P < 0.01$), MDS-UPDRS-III total score ($z_{16} = -3.530$, $P < 0.001$), posture and gait sub-score ($z_{16} = -3.423$, $P < 0.01$), and bradykinesia sub-score ($t_{16} = -5.156$, $P < 0.001$) over one year.

Across Parkinsonian disorders, there were significant group differences for the 1-year change in MDS-UPDRS-III total score ($F_{2,62} = 3.528$, $P < 0.05$), the bradykinesia sub-score ($F_{2,62} = 3.308$, $P < 0.05$), posture and gait sub-score ($F_{2,62} = 10.983$, $P < 0.001$), and Hoehn and Yahr stage (*Welch's* $F_{2,62} = 5.404$, $P < 0.05$). In particular, PSP had a greater increase in MDS-UPDRS-III total score ($P < 0.05$) and bradykinesia sub-score ($P < 0.05$) over one year compared to PD, and a greater 1-year increased in the posture and gait sub-score ($P < 0.01$) and Hoehn and Yahr stage ($P < 0.05$) compared to both PD and MSAp.

3.2. Progression effects in white matter tracts

All diffusion imaging tract-based means at baseline and 1-year are reported in the Supplemental material for fixel-based analysis (Supplemental Table 2), NODDI (Supplemental Table 3), and free-water imaging (Supplemental Table 4). There was no significant effect of the site covariate in any tract of interest for any of the diffusion imaging measures ($P_{FDR} > 0.05$).

3.2.1. Fixel-based analysis

There was a significant between-group difference in longitudinal FD 1-year change in several TCATT, SMATT, and subcortical tracts ($P_{FDR} < 0.05$) (Table 2). FD decreased more over one year in PD compared with healthy controls in the primary motor SMATT ($P^{FDR} < 0.05$) and the corticostriatal tract ($P^{FDR} < 0.05$) (Fig. 1A). In MSAp, FD declined in the primary motor SMATT ($P^{FDR} < 0.05$), pre-supplementary motor area SMATT ($P^{FDR} < 0.05$), somatosensory SMATT ($P^{FDR} < 0.05$), and the corticostriatal tract ($P^{FDR} < 0.05$) relative to controls, as well as the dorsal premotor SMATT ($P < 0.05$) and supplementary motor area SMATT ($P^{FDR} < 0.05$) relative to controls and PD (Fig. 1B). In PSP, FD declined more in the primary motor TCATT ($P < 0.01$) and somatosensory TCATT ($P^{FDR} < 0.05$) relative to controls, increased more in the dorsal and ventral premotor area TCATT ($P < 0.05$) relative to controls and PD, as well as in pre-supplementary motor area TCATT ($P^{FDR} < 0.01$) relative to controls, PD, and MSAp (Fig. 1C). In addition, PSP had a greater decline in FD in the primary motor ($P < 0.01$), dorsal and ventral premotor SMATT ($P^{FDR} < 0.05$), supplementary motor area SMATT ($P^{FDR} < 0.05$), and the corticostriatal tract ($P^{FDR} < 0.01$) compared with controls, and a greater decline in FD in the subthalamic nucleus to globus pallidus tract

Table 2
Fixel-Based Analysis in White Matter Tracts.

Tract of Interest	P-value FDR corrected	P-value uncorrected	F	Partial Eta Squared
Fibre Density (FD)				
M1 TCATT	**0.022**[d]	**0.007**	4.350	0.145
PMd TCATT	**0.020**[d,e]	**0.007**	4.400	0.146
PMv TCATT	**0.020**[d,e]	**0.006**	4.487	0.149
preSMA TCATT	**0.020**[d,e,f]	**0.004**	4.923	0.161
SMA TCATT	0.088	0.078	2.362	0.084
S1 TCATT	**0.033**[d]	**0.021**	3.435	0.118
M1 SMATT	**0.020**[a,b,d]	**0.005**	4.556	0.151
PMd SMATT	**0.032**[b,c,d]	**0.019**	3.531	0.121
PMv SMATT	**0.046**[d]	**0.035**	3.013	0.105
preSMA SMATT	**0.032**[b]	**0.018**	3.540	0.121
SMA SMATT	**0.021**[b,c,d]	**0.010**	4.061	0.137
S1 SMATT	**0.046**[b]	**0.033**	3.074	0.107
Nigrostriatal	0.087	0.072	2.420	0.086
Corticostriatal	**0.020**[a,b,d]	**0.004**	4.791	0.157
STN to GP	**0.021**[e,f]	**0.010**	4.058	0.137
MCP	0.167	0.157	1.787	0.065
SCP	0.210	0.210	1.544	0.057
Fibre Cross-section (log FC)				
M1 TCATT	0.300	0.105	2.116	0.076
PMd TCATT	0.193	**0.034**	3.034	0.106
PMv TCATT	0.300	0.159	1.777	0.065
preSMA TCATT	0.300	0.107	2.101	0.076
SMA TCATT	0.193	**0.026**	3.247	0.112
S1 TCATT	0.377	0.355	1.098	0.041
M1 SMATT	0.300	0.194	1.608	0.059
PMd SMATT	0.307	0.231	1.463	0.054
PMv SMATT	0.667	0.667	0.524	0.020
preSMA SMATT	0.307	0.267	1.343	0.050
SMA SMATT	0.300	0.194	1.608	0.059
S1 SMATT	0.307	0.271	1.329	0.049
Nigrostriatal	0.300	0.081	2.331	0.083
Corticostriatal	0.300	0.168	1.730	0.063
STN to GP	0.300	0.144	1.857	0.067
MCP	0.307	0.270	1.334	0.049
SCP	0.193	**0.024**	3.333	0.115
Fibre Density and Cross-section (FDC)				
M1 TCATT	0.140	0.114	2.046	0.074
PMd TCATT	0.075	**0.009**	4.160	0.139
PMv TCATT	0.075	**0.020**	3.469	0.119
preSMA TCATT	0.104	**0.043**	2.855	0.100
SMA TCATT	0.088	**0.031**	3.119	0.108
S1 TCATT	0.419	0.394	1.008	0.038
M1 SMATT	0.140	0.115	2.045	0.074
PMd SMATT	0.121	0.078	2.356	0.084
PMv SMATT	0.440	0.440	0.911	0.034
preSMA SMATT	0.106	0.050	2.728	0.096
SMA SMATT	0.121	0.076	2.385	0.085
S1 SMATT	0.149	0.131	1.933	0.070
Nigrostriatal	0.075	0.011	3.937	0.133
Corticostriatal	0.140	0.113	2.058	0.074
STN to GP	0.075	**0.015**	3.730	0.127
MCP	0.075	**0.022**	3.377	0.116
SCP	0.121	0.073	2.412	0.086

ANOVA results for main effect of group with age, sex, and site covariates.
Bold type indicates statistically significant values. Superscripts indicate significant post-hoc comparisons ($P < 0.05$, FDR-corrected).
TCATT: trans callosal tractography template, SMATT: sensorimotor area tract template, M1: Primary motor cortex, PMd: dorsal Premotor area, PMv: ventral Premotor area, SMA: supplementary motor area, S1: Primary sensory cortex, STN: subthalamic nucleus, GP: globus pallidus, MCP: middle cerebellar peduncle, SCP: superior cerebellar peduncle.

[a] PD vs. Controls.
[b] MSAp vs. Controls.
[c] MSAp vs. PD.
[d] PSP vs. Controls.
[e] PSP vs. PD.
[f] MSAp vs. PSP.

($P^{FDR} < 0.05$) compared with PD and MSAp. There were no differences between groups in any log-FC or FDC measures ($P^{FDR} > 0.05$).

3.2.2. Neurite Orientation dispersion and density imaging (NODDI)

There were no differences in longitudinal 1-year change in Viso, Vic, or ODI between groups in any of the white matter tracts ($P_{FDR} > 0.05$) (Table 3).

3.2.3. Free-water imaging

There were significant differences between groups in longitudinal 1-year change in FW in several TCATT, SMATT, and subcortical tracts for MSAp and PSP (Table 4). There were no differences in longitudinal progression effects in PD compared with healthy controls (Fig. 1D). MSAp had a greater increase in FW in the dorsal premotor ($P_{FDR} < 0.05$), pre-supplementary motor ($P^{FDR} < 0.05$), and supplementary motor area TCATT ($P^{FDR} < 0.05$), as well as the dorsal premotor ($P^{FDR} < 0.05$), pre-supplementary motor ($P^{FDR} < 0.05$), and supplementary motor area SMATT ($P^{FDR} < 0.05$) tracts compared with healthy controls and PD (Fig. 1E). PSP had greater increase in FW in the dorsal premotor area TCATT ($P^{FDR} < 0.05$), supplementary motor area TCATT ($P^{FDR} < 0.05$) and supplementary motor area SMATT ($P^{FDR} < 0.05$) relative to controls and PD (Fig. 1F). In addition, PSP had greater FW increase in the pre-supplementary motor TCATT ($P^{FDR} < 0.05$) and the pre-supplementary motor SMATT ($P^{FDR} < 0.05$) tracts relative to controls. Subcortically, PSP had a greater increase in FW in the nigrostriatal tract ($P^{FDR} < 0.05$) and subthalamic nucleus to globus pallidus tract ($P^{FDR} < 0.05$) relative to healthy controls, PD, and MSAp. There were no differences in FAt change between groups in any white matter tracts ($P^{FDR} > 0.05$).

3.3. Progression effects in gray matter regions

All diffusion imaging region-based means at baseline and one year are reported in the Supplemental material for NODDI (Supplemental Table 5), and free-water imaging (Supplemental Table 6). There was no significant effect of the site covariate in any region of interest for any of the diffusion imaging measures ($P_{FDR} > 0.05$).

3.3.1. Neurite orientation dispersion and density imaging (NODDI)

In gray matter regions, there was a significant difference in longitudinal 1-year change in Viso in the anterior substantia nigra and red nucleus, as well as 1-year change in Vic in the caudate nucleus and globus pallidus for PSP and MSAp ($P_{FDR} < 0.01$) (Table 5). In PSP, the anterior substantia nigra ($P^{FDR} < 0.01$) and red nucleus ($P^{FDR} < 0.01$) had greater 1-year change in Viso compared with controls, PD, and MSAp (Fig. 2A). Vic in the globus pallidus ($P^{FDR} < 0.05$) increased more over one year in PSP and MSAp relative to controls and PD (Fig. 2B). Vic also increased more over one year in the caudate nucleus ($P^{FDR} < 0.05$) in PSP relative to controls and PD. There were no differences in ODI change between groups ($P^{FDR} > 0.05$).

3.3.2. Free-water imaging

1-year change in FW in gray matter regions differed between groups in the putamen, caudate, subthalamic nucleus, red nucleus, and pedunculopontine nucleus (Table 6). In MSAp, FW increased more in the putamen ($P_{FDR} < 0.01$) compared with controls, PD, and PSP (Fig. 2C). In PSP, FW increased more in the red nucleus ($P^{FDR} < 0.05$) compared with controls and PD, as well as the subthalamic nucleus ($P^{FDR} < 0.001$) and pedunculopontine nucleus ($P^{FDR} < 0.01$) compared to controls, PD, and MSAp. There was greater FAt change for MSAp in the putamen ($P^{FDR} < 0.05$) compared to controls, PD, and PSP (Fig. 2D). PSP had greater 1-year FAt change in the anterior and posterior substantia nigra ($P^{FDR} < 0.01$), and subthalamic nucleus ($P^{FDR} < 0.01$) compared to controls, PD, and MSAp, and in the putamen ($P^{FDR} < 0.05$), red nucleus ($P^{FDR} < 0.01$)

Table 3
NODDI Imaging in White Matter Tracts.

Tract of Interest	P-value FDR corrected	P-value uncorrected	F	Partial Eta Squared
Isotropic Volume Fraction (Viso)				
M1 TCATT	0.397	0.123	1.984	0.072
PMd TCATT	0.397	0.079	2.351	0.084
PMv TCATT	0.397	0.123	1.989	0.072
preSMA TCATT	0.397	0.185	1.649	0.060
SMA TCATT	0.397	0.088	2.261	0.081
S1 TCATT	0.439	0.303	1.233	0.046
M1 SMATT	0.439	0.310	1.214	0.045
PMd SMATT	0.540	0.422	0.948	0.036
PMv SMATT	0.397	0.210	1.542	0.057
preSMA SMATT	0.397	0.195	1.605	0.059
SMA SMATT	0.540	0.445	0.900	0.034
S1 SMATT	0.817	0.817	0.311	0.012
Nigrostriatal	0.817	0.775	0.370	0.014
Corticostriatal	0.400	0.235	1.449	0.053
STN to GP	0.397	0.188	1.635	0.060
MCP	0.561	0.495	0.805	0.030
SCP	0.397	**0.028**	3.203	0.111
Orientation Dispersion Index (ODI)				
M1 TCATT	0.272	0.080	2.337	0.083
PMd TCATT	0.272	**0.033**	3.063	0.107
PMv TCATT	0.811	0.763	0.386	0.015
preSMA TCATT	0.272	0.073	2.411	0.086
SMA TCATT	0.051	**0.003**	5.135	0.167
S1 TCATT	0.287	0.152	1.810	0.066
M1 SMATT	0.276	0.130	1.941	0.070
PMd SMATT	0.276	0.123	1.987	0.072
PMv SMATT	0.545	0.449	0.892	0.034
preSMA SMATT	0.272	0.048	2.754	0.097
SMA SMATT	0.356	0.230	1.466	0.054
S1 SMATT	0.545	0.449	0.892	0.034
Nigrostriatal	0.276	0.106	2.107	0.076
Corticostriatal	0.545	0.399	0.997	0.037
STN to GP	0.756	0.667	0.524	0.020
MCP	0.923	0.923	0.160	0.006
SCP	0.311	0.183	1.658	0.061
Intracellular Volume Fraction (Vic)				
M1 TCATT	0.868	0.842	0.277	0.011
PMd TCATT	0.868	0.524	0.753	0.029
PMv TCATT	0.868	0.349	1.114	0.042
preSMA TCATT	0.868	0.449	0.892	0.034
SMA TCATT	0.868	0.733	0.429	0.016
S1 TCATT	0.868	0.755	0.397	0.015
M1 SMATT	0.868	0.868	0.240	0.009
PMd SMATT	0.868	0.855	0.259	0.010
PMv SMATT	0.868	0.156	1.789	0.065
preSMA SMATT	0.868	0.744	0.413	0.016
SMA SMATT	0.868	0.685	0.498	0.019
S1 SMATT	0.868	0.576	0.665	0.025
Nigrostriatal	0.868	0.606	0.616	0.023
Corticostriatal	0.868	0.692	0.487	0.019
STN to GP	0.868	0.770	0.376	0.014
MCP	0.868	0.193	1.615	0.059
SCP	0.868	0.297	1.251	0.046

ANOVA results for main effect of group with age, sex, and site covariates.
Bold type indicates statistically significant values. Superscripts indicate significant post-hoc comparisons (P < 0.05, FDR-corrected).
TCATT: trans callosal tractography template, SMATT: sensorimotor area tract template, M1: Primary motor cortex, PMd: dorsal Premotor area, PMv: ventral Premotor area, SMA: supplementary motor area, S1: Primary sensory cortex, STN: subthalamic nucleus, GP: globus pallidus, MCP: middle cerebellar peduncle, SCP: superior cerebellar peduncle.
[a]PD vs. Controls.
[b]MSAp vs. Controls.
[c]MSAp vs. PD.
[d]PSP vs. Controls.
[e]PSP vs. PD.
[f]MSAp vs. PSP.

Table 4
Free-Water Imaging in White Matter Tracts.

Tract of Interest	P-value FDR corrected	P-value uncorrected	F	Partial Eta Squared
Free-water (FW)				
M1 TCATT	0.121	0.089	2.253	0.080
PMd TCATT	**0.028**[b,c,d,e]	**0.013**	3.812	0.128
PMv TCATT	0.116	0.073	2.411	0.085
preSMA TCATT	**0.028**[b.c.d]	**0.011**	3.937	0.132
SMA TCATT	**0.028**[b,c,d,e]	**0.005**	4.598	0.150
S1 TCATT	0.116	0.075	2.393	0.084
M1 SMATT	0.121	0.114	2.047	0.073
PMd SMATT	**0.028**[b,c]	**0.011**	3.942	0.132
PMv SMATT	0.121	0.107	2.103	0.075
preSMA SMATT	**0.028**[b,d]	**0.012**	3.909	0.131
SMA SMATT	**0.028**[b,c,d,e]	**0.002**	5.235	0.168
S1 SMATT	0.121	0.103	2.133	0.076
Nigrostriatal	**0.028**[d,e,f]	**0.009**	4.124	0.137
Corticostriatal	0.116	0.075	2.388	0.084
STN to GP	**0.028**[d,e,f]	**0.010**	4.072	0.135
MCP	0.121	0.099	2.165	0.077
SCP	0.172	0.172	1.707	0.062
Free-water corrected Fractional Anisotropy (FAt)				
M1 TCATT	0.654	0.087	2.271	0.080
PMd TCATT	0.654	0.172	1.711	0.062
PMv TCATT	0.654	0.407	0.979	0.036
preSMA TCATT	0.654	0.220	1.503	0.055
SMA TCATT	0.654	0.028	3.198	0.110
S1 TCATT	0.654	0.260	1.363	0.050
M1 SMATT	0.654	0.477	0.838	0.031
PMd SMATT	0.710	0.710	0.462	0.017
PMv SMATT	0.654	0.443	0.904	0.034
preSMA SMATT	0.654	0.579	0.660	0.025
SMA SMATT	0.654	0.316	1.198	0.044
S1 SMATT	0.654	0.315	1.200	0.044
Nigrostriatal	0.654	0.036	3.001	0.103
Corticostriatal	0.654	0.521	0.759	0.028
STN to GP	0.654	0.072	2.421	0.085
MCP	0.654	0.233	1.456	0.053
SCP	0.654	0.125	1.974	0.071

ANOVA results for main effect of group with age, sex, and site covariates.
Bold type indicates statistically significant values. Superscripts indicate significant post-hoc comparisons (P < 0.05, FDR-corrected).
TCATT: trans callosal tractography template, SMATT: sensorimotor area tract template, M1: Primary motor cortex, PMd: dorsal Premotor area, PMv: ventral Premotor area, SMA: supplementary motor area, S1: Primary sensory cortex, STN: subthalamic nucleus, GP: globus pallidus, MCP: middle cerebellar peduncle, SCP: superior cerebellar peduncle.
[a]PD vs. Controls.
[b]MSAp vs. Controls.
[c]MSAp vs. PD.
[d]PSP vs. Controls.
[e]PSP vs. PD.
[f]MSAp vs. PSP.

and pedunculopontine nucleus ($P^{FDR} < 0.05$) compared to controls and PD.

3.4. Changes in diffusion measures associated with clinical disease progression

The fixel-based, free-water, and NODDI regions with significant change were entered into a backwards stepwise multiple regression to determine their association with change in MDS-UPDRS-III total score and bradykinesia sub-score over one year, across all Parkinsonian groups Fixel-based analysis variables did not significantly predict change in MDS-UPDRS-III total score ($R^2_{4,63} = 12.9\%$, $P = 0.083$), but did predict change in bradykinesia sub-score, with the final model including the somatosensory SMATT tract FD ($R^2_{1,63} = 14.2\%$, $P < 0.01$). For NODDI, the anterior substantia nigra Viso was the only variable included in the final models for predicting MDS-UPDRS-III total score

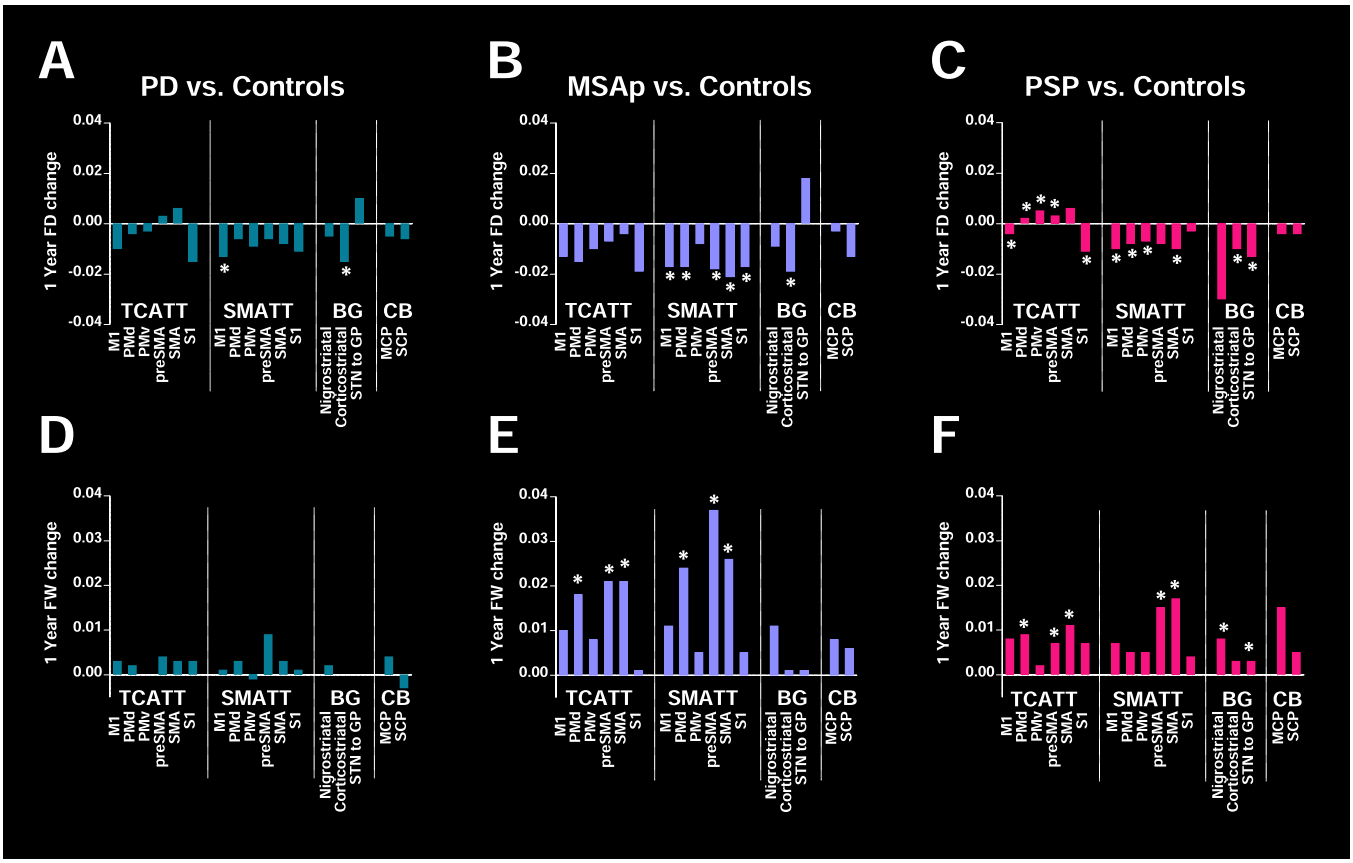

Fig. 1. Significant White Matter Tracts Fixel-Based Analysis and Free-Water Imaging. 1-year change in Fiber Density (FD) relative to control subjects for (**A**) PD, (**B**) MSAp, and (**C**) PSP. 1-year change in free-water (FW) relative to control subjects for (**D**) PD, (**E**) MSAp, and (**F**) PSP. *indicates significant post-hoc tests ($P_{FDR} < 0.05$). TCATT: Trans callosal tractography template, SMATT: sensorimotor area tract template, BG: basal ganglia tracts, CB: cerebellar tracts, M1: primary motor cortex, PMd: dorsal premotor area, PMv: ventral premotor area, SMA: supplementary motor area, S1: primary sensory cortex, STN: subthalamic nucleus, GP: globus pallidus, MCP: middle cerebellar peduncle, SCP: superior cerebellar peduncle.

($R^2_{1,63} = 7.4\%$, $P < 0.05$) and bradykinesia sub-score ($R^2_{1,63} = 7.6\%$, $P < 0.05$). Free-water variables significantly predicted change in MDS-UPDRS-III total score, with the final model including pre-supplementary motor area SMATT FW, supplementary motor area SMATT FW, Nigrostriatal FW, Putamen FAt, and pedunculopontine nucleus FW ($R^2_{5,64} = 27.8\%$, $P < 0.001$). In addition, free-water variables also predicted change in MDS-UPDRS-III bradykinesia sub-score, with the final model including pedunculopontine nucleus FW and putamen FAt ($R^2_{5,64} = 17.0\%$, $P < 0.01$).

4. Discussion

This multi-site cohort study applied multiple advanced diffusion imaging methods to investigate longitudinal 1-year changes in widespread white matter tracts and gray matter regions in PD and atypical Parkinsonian syndromes in a multi-site cohort. Fixel-based analysis and free-water imaging revealed longitudinal declines in a greater number of descending sensorimotor tracts in MSAp and PSP compared to PD. In contrast, only the primary motor descending sensorimotor tract had progressive decline in FD over one year in PD. All Parkinsonian syndromes had reduced FD longitudinally over one year in the corticostriatal tract when compared to controls. Second, fixel-based analysis revealed significant longitudinal changes in multiple transcallosal tracts (primary motor, dorsal and ventral premotor, pre-supplementary motor, and supplementary motor area) in PSP compared with that in MSAp and PD. Third, in gray matter regions, FW and FAt showed longitudinal changes over one year in the same regions demonstrating impairment in previous cross-sectional studies in MSAp (putamen) and PSP (substantia nigra, putamen, subthalamic nucleus, red nucleus, and pedunculopontine nucleus). Finally, across all three Parkinsonian disorders, the three diffusion methods were associated with change in clinical disease severity. These results identify nigrostriatal regions with progression effects and emphasize the importance of extra-striatal and extra-nigral regions in tracking disease progression in atypical Parkinsonian syndromes.

PSP is an atypical Parkinsonism with early clinical signs of posture and gait disturbances that is characterized by pathology in the substantia nigra, globus pallidus, subthalamic nucleus, pons, and cerebellum (Dickson, 2012; Ahmed et al., Feb 2008; Halliday et al., Oct 2005). There is also pathology within the primary motor and supplementary motor cortical areas and in corticocortical projections (Halliday et al., Oct 2005). The fixel-based analysis findings are in line with this pathology and showed that sensorimotor corticospinal tracts had progressive reductions in FD over one year in PSP and a greater number of transcallosal tracts had progression effects compared with PD and MSAp. These results extend previous cross-sectional fixel-based analysis that revealed the corpus callosum had reduced FD in PSP compared to both PD and MSAp (Nguyen et al., 2021). Consistent with these cross-sectional findings, in the current study there was longitudinal reduction in FD in the primary motor and somatosensory transcallosal tracts. In comparison, FD increased longitudinally in the dorsal and ventral premotor and pre-supplementary motor area transcallosal tracts. Increased FD in these specific tracts was unexpected and contradictory to the aforementioned cross-sectional study where the entire corpus callosum was affected broadly. Moreover, these findings support that the primary motor and somatosensory corpus callosum are promising

Table 5
NODDI Imaging in Gray Matter Regions.

Region of Interest	P-value FDR corrected	P-value uncorrected	F	Partial Eta Squared
Isotropic Volume Fraction (Viso)				
aSN	**0.020**[d,e,f]	**0.003**	5.171	0.168
pSN	0.107	**0.028**	3.187	0.110
PUT	0.107	**0.039**	2.924	0.102
CN	0.117	0.063	2.530	0.090
GP	0.147	0.101	2.145	0.077
STN	0.644	0.594	0.636	0.024
RN	**<0.001**[d,e,f]	**0.000**	6.640	0.206
THA	0.592	0.501	0.794	0.030
PPN	0.107	0.041	2.881	0.101
DN	0.111	0.051	2.708	0.095
VER	0.685	0.685	0.498	0.019
LB V	0.157	0.121	2.001	0.072
LB VI	0.147	0.102	2.143	0.077
Orientation Dispersion Index (ODI)				
aSN	0.541	0.096	2.187	0.079
pSN	0.816	0.634	0.573	0.022
PUT	0.894	0.888	0.211	0.008
CN	0.816	0.547	0.713	0.027
GP	0.541	0.059	2.582	0.091
STN	0.894	0.894	0.203	0.008
RN	0.816	0.635	0.573	0.022
THA	0.541	0.208	1.553	0.057
PPN	0.816	0.690	0.490	0.019
DN	0.541	0.193	1.613	0.059
VER	0.816	0.516	0.768	0.029
LB V	0.541	0.129	1.948	0.071
LB VI	0.816	0.399	0.998	0.037
Intracellular Volume Fraction (Vic)				
aSN	0.179	0.069	2.466	0.088
pSN	0.835	0.642	0.561	0.021
PUT	0.169	**0.039**	2.919	0.102
CN	**0.026**[d,e]	**0.004**	4.860	0.159
GP	**0.026**[b,c,d,e]	**0.002**	5.430	0.175
STN	0.960	0.932	0.146	0.006
RN	0.457	0.281	1.298	0.048
THA	0.960	0.932	0.146	0.006
PPN	0.282	0.130	1.938	0.070
DN	0.960	0.960	0.100	0.004
VER	0.299	0.161	1.763	0.064
LB V	0.458	0.317	1.197	0.045
LB VI	0.179	0.066	2.500	0.089

ANOVA results for main effect of group with age, sex, and site covariates.
Bold type indicates statistically significant values. Superscripts indicate significant post-hoc comparisons ($P < 0.05$, FDR-corrected).
aSN: anterior substantia nigra, pSN: posterior substantia nigra, PUT: putamen, CN: caudate nucleus, GP: globus pallidus, STN: subthalamic nucleus, RN: red nucleus, THA: thalamus, PPN: pedunculopontine nucleus, DN: dentate nucleus, LB V: cerebellar lobule V, LB VI: cerebellar lobule VI, VER: the cerebellar vermis.
[a]PD vs. Controls.
[b]MSAp vs. Controls.
[c]MSAp vs. PD.
[d]PSP vs. Controls.
[e]PSP vs. PD.
[f]MSAp vs. PSP.

sites to track longitudinal progression of FD in PSP. Free-water imaging also revealed pre-supplementary, and supplementary motor area sensorimotor and transcallosal tracts had increased FW over one year in PSP. Further, FW and FAt increased over one year in other disease relevant regions, including the substantia nigra, putamen, subthalamic nucleus, red nucleus, and pedunculopontine nucleus. Here, increased FAt in gray matter can indicate gliosis and it is also possible a loss of cell bodies could lead to a reduction in the isotropy of diffusion (Budde et al., Aug 2011). NODDI has previously shown widespread PSP-related pathology across the basal ganglia, midbrain, pons, cerebellum, and cortical regions in cross-sectional studies (Planetta et al., Feb 2016; Mitchell et al., 2019; Mak et al., 2021). In the current study, progression effects in PSP were observed in limited regions with NODDI in the anterior substantia nigra, basal ganglia, and midbrain. In contrast, fixel-based analysis and free-water imaging detected widespread longitudinal progression effects over one year in several transcallosal tracts as well as key disease-relevant gray matter regions in PSP.

Cross-sectional diffusion imaging studies highlight the superior cerebellar peduncle as an important structure affected in PSP (Planetta et al., Feb 2016; Mitchell et al., 2019; Tsuboi et al., 2003). This structure also has shown progression effects with single-tensor diffusion MRI and volumetric MRI (Dutt et al., 2016; Zhang et al., 2016). In the current study, there was cross-sectional impairment of the superior cerebellar peduncle in PSP with all three diffusion methods, but there were no progression effects. This suggests that this structure degenerated earlier in the disease. The midbrain longitudinal changes detected by NODDI and free-water in the current study are in line with volumetric MRI findings that show midbrain atrophy is a marker of progression in PSP (Whitwell et al., 2019). This volumetric MRI marker has shown to outperform PET imaging of tau deposition as a longitudinal marker and the current results corroborate the midbrain as an important site of progression in PSP (Whitwell et al., 2019).

MSAp is characterized by pathology frequently in the nigrostriatal and olivopontocerebellar systems, the putamen, caudate, globus pallidus, substantia nigra, cerebellum, and sometimes in the thalamus, corticospinal tracts, and anterior cingulate cortex (Cykowski et al., Aug 2015; Wenning et al., Mar 1997). Our findings are consistent with pathology and reveal longitudinal decline in FD in several corticospinal sensorimotor tracts in MSAp. FD in the corticospinal tract has been shown to be impaired in MSAp compared to PD in cross-sectional studies (Nguyen et al., 2021). Free-water imaging also revealed dorsal premotor, pre-supplementary, and supplementary motor area sensorimotor and transcallosal tracts had increased FW over one year. Further, FW and FAt increased over one year in the putamen, which is a region known to be implicated in MSAp (Planetta et al., Feb 2016; Mitchell et al., 2019; Barbagallo et al., 2016; Baudrexel et al., 2014; Ito et al., Jul 2007; Köllensperger et al., 2007; Tsukamoto et al., 2012). NODDI revealed there was longitudinal increased in Vic in the globus pallidus which was previously found to be affected cross-sectionally compared to controls (Mitchell et al., 2019). Cross-sectional diffusion imaging also reveals the importance of the middle cerebellar peduncle in distinguishing MSAp from PD and PSP (Planetta et al., Feb 2016; Mitchell et al., 2019; Nicoletti et al., Oct 2006; Sako et al., 2016). The middle cerebellar peduncle had no progression effects in MSAp in the current cohort, even though there were cross-sectional effects detected by all three diffusion methods. This could suggest it undergoes degeneration earlier or these methods cannot detect longitudinal changes in peduncles.

PD is primarily defined by nigrostriatal pathology (Braak et al., 2003; Fearnley and Lees, Oct 1991). Our results demonstrated that in PD there was reduced FD in the primary motor sensorimotor tract. This is not surprising since there is reduced functional activity in the primary motor cortex in PD (Burciu and Vaillancourt, Nov 2018). In contrast to our results, a previous fixel-based analysis demonstrated longitudinal changes in FD and log-FC in the corpus callosum in PD (Rau et al., 2019). Notably, their cohort had a longer disease duration (6.8 years) compared with our study (4.5 years). In addition, atypical Parkinsonian disorders had more impairment in transcallosal tracts in the current cohort. Thus, it is likely that corpus callosum neurodegeneration is associated with even more advanced and severe Parkinsonism. We did not detect progression effects in the substantia nigra with any diffusion method which has been previously found in the posterior substantia nigra in early PD and anterior substantia nigra in moderate- to late-stage PD (Mitchell et al., 2021). In the current cohort, we did find elevated FW and Viso in the posterior substantia nigra of PD cross-sectionally compared with controls, and thus it is most likely that extracellular fluid had already increased to a plateau and the 1-year time frame used here was not sufficient for the more advanced disease stage of this PD cohort (4.5 years). Prior studies have consistently found that early-stage PD has

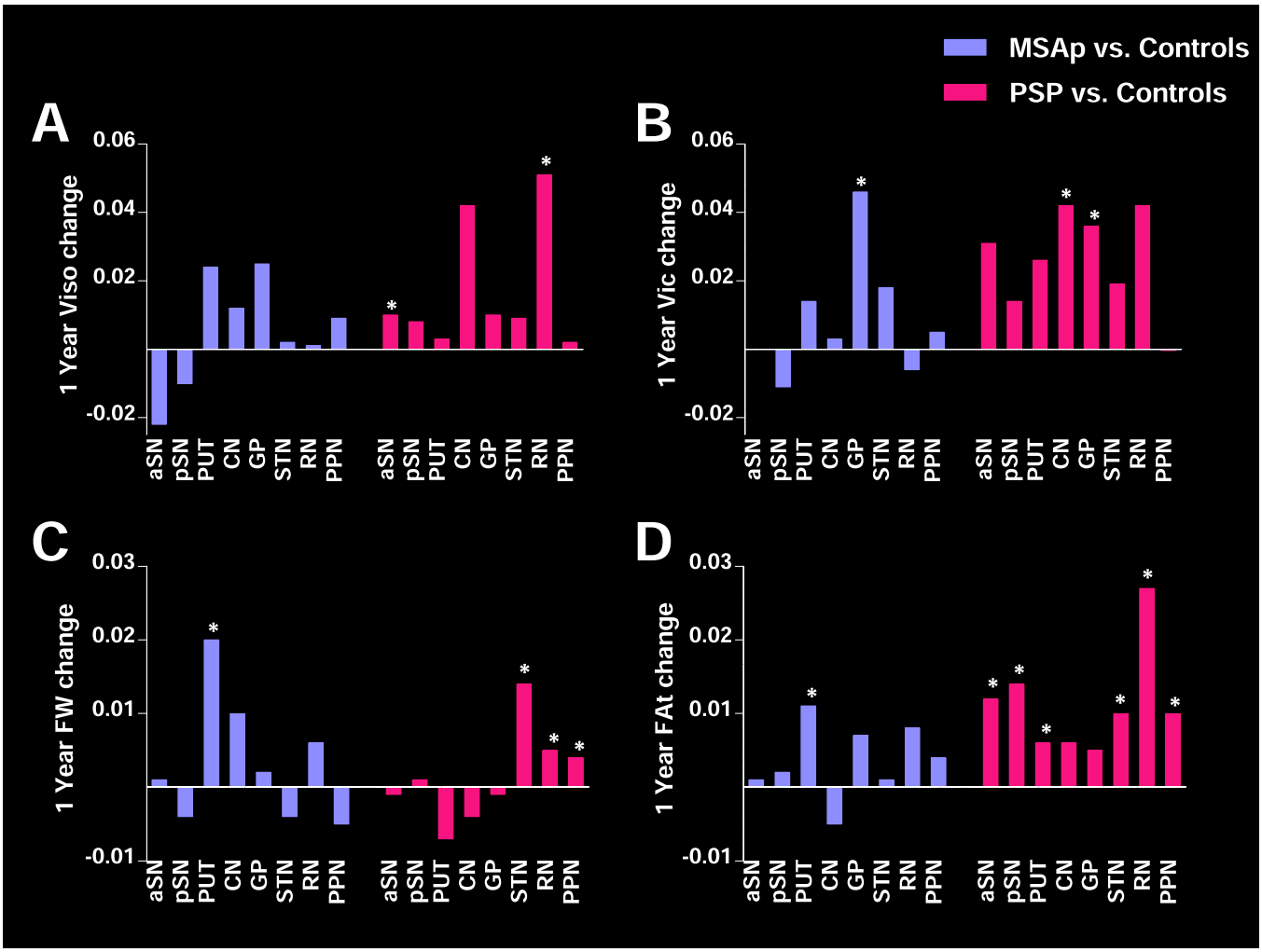

Fig. 2. Significant Gray Matter Regions for NODDI and Free-water Imaging. 1-year change in NODDI variables, (**A**) isotropic volume fraction (Viso) and (**B**) intracellular volume fraction (Vic) for MSAp (purple) and progressive supranuclear palsy (pink) relative to healthy controls subjects. 1-year change in free-water Imaging variables, (**C**) Free-water (FW) and (**D**) FW corrected fractional anisotropy (FAt) for MSAp (purple) and progressive supranuclear palsy (pink) relative to healthy controls subjects. *indicates significant post-hoc tests ($P_{FDR} < 0.05$). aSN: anterior substantia nigra, pSN: posterior substantia nigra, PUT: putamen, CN: caudate nucleus, GP: globus pallidus, STN: subthalamic nucleus, RN: red nucleus, PPN: pedunculopontine nucleus. (For interpretation of the references to colour in this figure legend, the reader is referred to the web version of this article.)

increased nigral FW longitudinally (Burciu et al., 2017; Ofori et al., 2015). Furthermore, there was reduced FD over one year in the corticostriatal tract in the current study in PD, MSAp, and PSP. These findings are consistent with longitudinal task-based functional MRI that showed reduced signal over one year in the putamen and primary motor cortex for PD, MSAp, and PSP, with atypical Parkinsonian disorders additionally reducing signal in the supplementary motor area and superior cerebellum (Burciu et al., 2016). Overall, there were significantly less progression effects observed in PD compared with atypical Parkinsonian disorders, and PD related effects were restricted to primary motor cortical regions and striatum.

All three diffusion methods were associated with change in clinical disease severity across all three Parkinsonian syndromes highlighting key regions associated with motor progression. In fixel-based analysis, 1-year change in somatosensory SMATT FD significantly predicted 1-year change in MDS-UPDRS-III bradykinesia sub-score. With NODDI, Viso in the anterior substantia nigra predicted 1-year change in MDS-UPDRS-III total score and bradykinesia sub-score. These results support previous work demonstrating baseline FW in the substantia nigra predicted 1-year change in bradykinesia score, (Ofori et al., 2015) which has been replicated in a new cohort (Arpin, xxxx). With free-water imaging, pre-supplementary motor area SMATT FW, supplementary motor area SMATT FW, nigrostriatal FW, as well as putamen FAt, and pedunculopontine nucleus FW predicted 1-year change in MDS-UPDRS-III total score. In addition, pedunculopontine FW and putamen FAt also predicted 1-year change in MDS-UPDRS-III bradykinesia sub-score. The pedunculopontine nucleus has consistently shown to have increased FW in PSP, and the putamen has consistently shown increased FAt in MSAp (Planetta et al., Feb 2016; Mitchell et al., 2019). In the current study, FW in the pedunculopontine nucleus increased in PSP, and FAt in the putamen increased in MSAp longitudinally. Together, these results provide strong evidence that free-water imaging of the pedunculopontine nucleus and putamen is associated with more advanced forms of Parkinsonism. These set of findings provide a novel link between changes in each neuroimaging biomarker and clinical progression of motor symptoms. A limitation of this study is the low sample size in MSAp, although the findings were robust in this sample. In addition, it is possible that the large attrition rates in MSAp and PSP may present some bias in the clinical profile of the cohort who completed the follow up. Those that were lost to follow up tended to have higher disease severity, and rapid disease progression with substantial mortality rates.

NODDI imaging based on the current multi-shell scan did not detect any white matter tract progression effects and revealed few effects in gray matter regions across different Parkinsonian syndromes. Further,

Table 6
Free-water Imaging in Gray Matter Regions.

Region of Interest	P-value FDR corrected	P-value uncorrected	F	Partial Eta Squared
Free-water (FW)		**Subheadings can be merged across columns, in bold**[a]		
aSN	0.230	0.106	2.109	0.075
pSN	0.944	0.944	0.127	0.005
PUT	**0.007**[b,c,f]	**0.001**	5.841	0.183
CN	0.073	**0.028**	3.206	0.110
GP	0.570	0.307	1.222	0.045
STN	**<0.001**[d,e,f]	**<0.001**	20.190	0.437
RN	**0.026**[d,e]	**0.008**	4.276	0.141
THA	0.592	0.364	1.077	0.040
PPN	**0.009**[d,e,f]	**0.002**	5.223	0.167
DN	0.944	0.814	0.315	0.012
VER	0.703	0.487	0.819	0.031
LB V	0.768	0.591	0.642	0.024
LB VI	0.944	0.885	0.216	0.008
Free-water corrected Fractional Anisotropy (FAt)				
aSN	**0.009**[d,e,f]	**0.002**	5.333	0.170
pSN	**0.010**[d,e,f]	**0.003**	5.180	0.166
PUT	**<0.001**[b,c,d,e,f]	**0.000**	8.713	0.251
CN	0.067	**0.036**	2.980	0.103
GP	0.424	0.359	1.090	0.040
STN	**0.009**[d,e,f]	**0.002**	5.217	0.167
RN	**0.026**[d,e]	**0.010**	4.047	0.135
THA	0.142	0.099	2.160	0.077
PPN	**0.037**[d,e]	**0.017**	3.608	0.122
DN	0.434	0.401	0.993	0.037
VER	0.081	0.050	2.724	0.095
LB V	0.142	0.109	2.088	0.074
LB VI	0.483	0.483	0.827	0.031

ANOVA results for main effect of group with age, sex, and site covariates.
Bold type indicates statistically significant values. Superscripts indicate significant post-hoc comparisons ($P < 0.05$, FDR-corrected).
aSN: anterior substantia nigra, pSN: posterior substantia nigra, PUT: putamen, CN: caudate nucleus, GP: globus pallidus, STN: subthalamic nucleus, RN: red nucleus, THA: thalamus, PPN: pedunculopontine nucleus, DN: dentate nucleus, LB V: cerebellar lobule V, LB VI: cerebellar lobule VI, VER: the cerebellar vermis.
[a] PD vs. Controls.
[b] MSAp vs. Controls.
[c] MSAp vs. PD.
[d] PSP vs. Controls.
[e] PSP vs. PD.
[f] MSAp vs. PSP.

the relationship between neurite density measured by Vic in NODDI and FD in Fixel based analysis has not been well established. The present study shows poor overlap between the two measures. A previous study that conducted NODDI and Fixel based analysis in a rat model of traumatic brain injury also showed a lack of agreement between the modalities.(Chary et al., 2021). It is possible that alternate multi-shell scan parameters would have better outcomes for the NODDI analysis.

5. Conclusions

In summary, fixel-based analysis based on a multi-shell scan and free-water imaging based on a single-shell scan were particularly sensitive to widespread longitudinal changes in atypical Parkinsonism. The present results identify novel extra-nigral and extra-striatal longitudinal progression effects in atypical Parkinsonism when applying multiple diffusion methods that are associated with clinical disease progression. Fixel-based analysis and free-water imaging are particularly sensitive to these longitudinal changes in atypical Parkinsonism. These findings are critical for future applications of neuroimaging biomarkers for tracking progression in Parkinsonian disorders, especially atypical Parkinsonian disorders that rely on rapid and early identification for early intervention and clinical trial participation.

Funding

This work was supported by the National Institutes of Health [U01 NS102038]. This work was supported in part by an NIH award, S10 OD021726, for High End Instrumentation. A portion of this work was performed in the McKnight Brain Institute at the National High Magnetic Field Laboratory's AMRIS Facility, which is supported by National Science Foundation Cooperative Agreement No. DMR-1644779 and the State of Florida. Parkinson's subjects were enrolled from several participating Parkinson's Foundation Centers of Excellence.

CRediT authorship contribution statement

Trina Mitchell: Formal analysis, Data curation, Writing – original draft, Visualization. **Bradley J. Wilkes:** Formal analysis, Software, Data curation, Writing – review & editing. **Derek B. Archer:** Software, Validation, Data curation, Writing – review & editing. **Winston T. Chu:** Software, Validation, Data curation, Writing – review & editing. **Stephen A. Coombes:** Methodology, Writing – review & editing. **Song Lai:** Methodology, Software, Writing – review & editing. **Nikolaus R. McFarland:** Conceptualization, Methodology, Writing – review & editing. **Michael S. Okun:** Conceptualization, Methodology, Writing – review & editing. **Mieniecia L. Black:** Investigation, Project administration. **Ellen Herschel:** Investigation, Project administration. **Tanya Simuni:** Methodology, Resources, Writing – review & editing. **Cynthia Comella:** Methodology, Resources, Writing – review & editing. **Mitra Afshari:** Methodology, Resources, Writing – review & editing. **Tao Xie:** Methodology, Resources, Writing – review & editing. **Hong Li:** Formal analysis, Validation. **Todd B. Parrish:** Methodology, Writing – review & editing. **Ajay S. Kurani:** Methodology, Writing – review & editing. **Daniel M. Corcos:** Conceptualization, Methodology, Writing – review & editing, Supervision. **David E. Vaillancourt:** Conceptualization, Methodology, Writing – review & editing, Supervision, Funding acquisition.

Declaration of Competing Interest

The authors declare the following financial interests/personal relationships which may be considered as potential competing interests: Dr. Derek B. Archer has received grant support from the Parkinson's Foundation. Dr. Nikolaus R. McFarland reports grants from the NIH and the Michael J. Fox Foundation, and has received personal honoraria from the NIH and the American Academy of Neurology. Dr. Michael S. Okun serves as consultant for the National Parkinson's Foundation, and has received research grants from the National Institutes of Health, National Parkinson's Foundation, Michael J. Fox Foundation, Parkinson Alliance, Smallwood Foundation, Bachmann-Strauss Foundation, Tourette Syndrome Association, and UF Foundation. Dr. Okun is an associate editor for New England Journal of Medicine Journal Watch Neurology. Dr. Tanya Simuni reports grants from NINDS, Michael J. Fox Foundation, Parkinson's Foundation, Biogen, Roche, Neuroderm, Sanofi, and Sun Pharma for research and clinical trials, and also served as a consultant for Michael J. Fox Foundation, Parkinson's Foundation, Acadia, Abbvie, Adamas, Anavex, Allergan, Accorda, Denali, Neuroderm, Neurocrine, Revance, Sanofi, Sunovion, TEVA, Takeda, Voyager, and US World Meds. Dr. Simuni has received honorarium from Acadia, Adamas, and TEVA. Dr. Cynthia Comella recieves research support from the NIH, Parkinson's Foundation, Dystonia Medical Research Foundation, Merz Pharmaceutical, Revance Therapeutic, Retrophin and Acorda Therapeutic, and has served as a consultant or an advisory committee member for Acorda Therapeutics, Allergan Inc, Lundbeck Ltd., Medtronic Inc., Merz Pharmaceuticals, Acadia Pharmaceuticals, Jazz Pharmaceuticals, Neurocrine Biosciences Inc., Revance Therapeutic,

Sunovion. Dr. Comella serves on the editorial board of Clinical Neuropharmacology and Sleep Medicine, and receives royalties from Cambridge, Wolters Kluwer. Dr. Mitra Afshari reports grants from the Parkinson's Foundation, Michael J. Fox Foundation, and the Anti-Aging Foundation of Chicago. Dr. Tao Xie has been funded by the Parkinson's Foundation, NIH, Michael J Fox Foundation for Parkinson's Research, Abbvie, Stoparkinson and Biohaven Pharmaceuticals for research and clinical trials, served as consultant for Parkinson's Foundation and CVS/Caremark, and served on the editorial board for the Translational Neurodegeneration. Dr. Daniel M. Corcos reports grants from NIH. Dr. David E. Vaillancourt reports grants from NIH, NSF, and Tyler's Hope Foundation during the conduct of the study, and personal honoraria from NIH and Parkinson's Foundation unrelated to the submitted work. All other authors report no disclosures.

Acknowledgements

We would like to sincerely thank all of the participants for their time and contributions to this research.

Appendix A. Supplementary data

Supplementary data to this article can be found online at https://doi.org/10.1016/j.nicl.2022.103022.

References

Dickson DW. Parkinson's disease and parkinsonism: neuropathology, Cold Spring Harb Perspect Med., Aug 1 2012; 2(8), 10.1101/cshperspect.a009258.

Ahmed, Z., Josephs, K.A., Gonzalez, J., DelleDonne, A., Dickson, D.W., Feb 2008. Clinical and neuropathologic features of progressive supranuclear palsy with severe pallido-nigro-luysial degeneration and axonal dystrophy. Brain. 131 (Pt 2), 460–472. https://doi.org/10.1093/brain/awm301.

Cykowski, M.D., Coon, E.A., Powell, S.Z., et al., Aug 2015. Expanding the spectrum of neuronal pathology in multiple system atrophy. Brain. 138 (Pt 8), 2293–2309. https://doi.org/10.1093/brain/awv114.

Wenning, G.K., Tison, F., Ben Shlomo, Y., Daniel, S.E., Quinn, N.P., Mar 1997. Multiple system atrophy: a review of 203 pathologically proven cases. Mov. Disord. 12 (2), 133–147. https://doi.org/10.1002/mds.870120203.

Halliday, G.M., Macdonald, V., Henderson, J.M., Oct 2005. A comparison of degeneration in motor thalamus and cortex between progressive supranuclear palsy and Parkinson's disease. Brain. 128 (Pt 10), 2272–2280. https://doi.org/10.1093/brain/awh596.

Planetta, P.J., Ofori, E., Pasternak, O., et al., Feb 2016. Free-water imaging in Parkinson's disease and atypical parkinsonism. Brain. 139 (Pt 2), 495–508. https://doi.org/10.1093/brain/awv361.

Mitchell, T., Archer, D.B., Chu, W.T., et al., 2019. Neurite orientation dispersion and density imaging (NODDI) and free-water imaging in Parkinsonism. Hum. Brain Mapp. 40 (17), 5094–5107. https://doi.org/10.1002/hbm.24760.

Burciu, R.G., Ofori, E., Archer, D.B., et al., 2017. Progression marker of Parkinson's disease: a 4-year multi-site imaging study. Brain. 140 (8), 2183–2192. https://doi.org/10.1093/brain/awx146.

Ofori, E., Krismer, F., Burciu, R.G., Pasternak, O., McCracken, J.L., Lewis, M.M., Du, G., McFarland, N.R., Okun, M.S., Poewe, W., Mueller, C., Gizewski, E.R., Schocke, M., Kremser, C., Li, H., Huang, X., Seppi, K., Vaillancourt, D.E., 2017. Free water improves detection of changes in the substantia nigra in parkinsonism: A multisite study. Mov. Disord. 32 (10), 1457–1464.

Raffelt, D.A., Tournier, J.-D., Smith, R.E., Vaughan, D.N., Jackson, G., Ridgway, G.R., Connelly, A., 2017. Investigating white matter fibre density and morphology using fixel-based analysis. Neuroimage. 144, 58–73.

Raffelt, D., Tournier, J.-D., Rose, S., Ridgway, G.R., Henderson, R., Crozier, S., Salvado, O., Connelly, A., 2012. Apparent Fibre Density: a novel measure for the analysis of diffusion-weighted magnetic resonance images. Neuroimage. 59 (4), 3976–3994.

Li, Y., Guo, T., Guan, X., Gao, T., Sheng, W., Zhou, C., Wu, J., Xuan, M., Gu, Q., Zhang, M., Yang, Y., Huang, P., 2020. Fixel-based analysis reveals fiber-specific alterations during the progression of Parkinson's disease. Neuroimage Clin. 27, 102355.

Rau, Y.-A., Wang, S.-M., Tournier, J.-D., Lin, S.-H., Lu, C.-S., Weng, Y.-H., Chen, Y.-L., Ng, S.-H., Yu, S.-W., Wu, Y.-M., Tsai, C.-C., Wang, J.-J., 2019. A longitudinal fixel-based analysis of white matter alterations in patients with Parkinson's disease. Neuroimage Clin. 24, 102098.

Nguyen, T.-T., Cheng, J.-S., Chen, Y.-L., Lin, Y.-C., Tsai, C.-C., Lu, C.-S., Weng, Y.-H., Wu, Y.-M., Hoang, N.-T., Wang, J.-J., 2021. Fixel-based analysis of white matter degeneration in patients with progressive supranuclear palsy or multiple system atrophy, as compared to parkinson's disease. Front. Aging Neurosci. 13, 625874 https://doi.org/10.3389/fnagi.2021.625874.

Zhang, H., Schneider, T., Wheeler-Kingshott, C.A., Alexander, D.C., 2012. NODDI: practical in vivo neurite orientation dispersion and density imaging of the human brain. Neuroimage. 61 (4), 1000–1016. https://doi.org/10.1016/j.neuroimage.2012.03.072.

Nazeri, A., Chakravarty, M.M., Rotenberg, D.J., Rajji, T.K., Rathi, Y., Michailovich, O.V., Voineskos, A.N., 2015. Functional consequences of neurite orientation dispersion and density in humans across the adult lifespan. J. Neurosci. 35 (4), 1753–1762.

Ofori, E., Pasternak, O., Planetta, P.J., Li, H., Burciu, R.G., Snyder, A.F., Lai, S., Okun, M.S., Vaillancourt, D.E., 2015. Longitudinal changes in free-water within the substantia nigra of Parkinson's disease. Brain. 138 (8), 2322–2331.

Pasternak, O., Sochen, N., Gur, Y., Intrator, N., Assaf, Y., Sep 2009. Free water elimination and mapping from diffusion MRI. Magn. Reson. Med. 62 (3), 717–730. https://doi.org/10.1002/mrm.22055.

Budde, M.D., Janes, L., Gold, E., Turtzo, L.C., Frank, J.A., Aug 2011. The contribution of gliosis to diffusion tensor anisotropy and tractography following traumatic brain injury: validation in the rat using Fourier analysis of stained tissue sections. Brain. 134 (Pt 8), 2248–2260. https://doi.org/10.1093/brain/awr161.

Hoglinger, G.U., Respondek, G., Stamelou, M., et al., Jun 2017. Clinical diagnosis of progressive supranuclear palsy: the movement disorder society criteria. Mov. Disord. 32 (6), 853–864. https://doi.org/10.1002/mds.26987.

Gilman, S., Wenning, G.K., Low, P.A., et al., 2008. Second consensus statement on the diagnosis of multiple system atrophy. Neurology. 71 (9), 670–676. https://doi.org/10.1212/01.wnl.0000324625.00404.15.

Hughes, A.J., Daniel, S.E., Kilford, L., Lees, A.J., Mar 1992. Accuracy of clinical diagnosis of idiopathic Parkinson's disease: a clinico-pathological study of 100 cases. J. Neurol. Neurosurg. Psychiatry 55 (3), 181–184.

Goetz, C.G., Fahn, S., Martinez-Martin, P., Poewe, W., Sampaio, C., Stebbins, G.T., Stern, M.B., Tilley, B.C., Dodel, R., Dubois, B., Holloway, R., Jankovic, J., Kulisevsky, J., Lang, A.E., Lees, A., Leurgans, S., LeWitt, P.A., Nyenhuis, D., Olanow, C.W., Rascol, O., Schrag, A., Teresi, J.A., Van Hilten, J.J., LaPelle, N., 2007. Movement disorder society-sponsored revision of the unified parkinson's disease rating scale (MDS-UPDRS): process, format, and clinimetric testing plan. Mov. Disord. 22 (1), 41–47.

Wenning, G.K., Tison, F., Seppi, K., Sampaio, C., Diem, A., Yekhlef, F., Ghorayeb, I., Ory, F., Galitzky, M., Scaravilli, T., Bozi, M., Colosimo, C., Gilman, S., Shults, C.W., Quinn, N.P., Rascol, O., Poewe, W., 2004. Development and validation of the Unified Multiple System Atrophy Rating Scale (UMSARS). Mov. Disord. 19 (12), 1391–1402.

Golbe, L.I., Ohman-Strickland, P.A., Jun 2007. A clinical rating scale for progressive supranuclear palsy. Brain. 130 (Pt 6), 1552–1565. https://doi.org/10.1093/brain/awm032.

Nasreddine, Z.S., Phillips, N.A., BÃ©dirian, V., Charbonneau, S., Whitehead, V., Collin, I., Cummings, J.L., Chertkow, H., 2005. The Montreal cognitive assessment, MoCA: a brief screening tool for mild cognitive impairment. J. Am. Geriatr. Soc. 53 (4), 695–699.

Smith, S.M., Jenkinson, M., Woolrich, M.W., Beckmann, C.F., Behrens, T.E.J., Johansen-Berg, H., Bannister, P.R., De Luca, M., Drobnjak, I., Flitney, D.E., Niazy, R.K., Saunders, J., Vickers, J., Zhang, Y., De Stefano, N., Brady, J.M., Matthews, P.M., 2004. Advances in functional and structural MR image analysis and implementation as FSL. Neuroimage. 23, S208–S219.

Andersson, J.L.R., Sotiropoulos, S.N., 2016. An integrated approach to correction for off-resonance effects and subject movement in diffusion MR imaging. Neuroimage. 125, 1063–1078. https://doi.org/10.1016/j.neuroimage.2015.10.019.

Veraart, J., Novikov, D.S., Christiaens, D., Ades-Aron, B., Sijbers, J., Fieremans, E., 2016. Denoising of diffusion MRI using random matrix theory. Neuroimage. 142, 394–406. https://doi.org/10.1016/j.neuroimage.2016.08.016.

Jeurissen, B., Tournier, J.D., Dhollander, T., Connelly, A., Sijbers, J., Dec 2014. Multi-tissue constrained spherical deconvolution for improved analysis of multi-shell diffusion MRI data. Neuroimage. 103, 411–426. https://doi.org/10.1016/j.neuroimage.2014.07.061.

Zarkali A, McColgan P, Leyland LA, Lees AJ, Weil RS. Visual dysfunction predicts cognitive impairment and white matter degeneration in parkinson's disease, Mov Disord., Jan 9 2021; 10.1002/mds.28477.

Zarkali, A., McColgan, P., Leyland, L.A., Lees, A.J., Weil, R.S., Feb 2022. Longitudinal thalamic white and grey matter changes associated with visual hallucinations in Parkinson's disease. J. Neurol. Neurosurg. Psychiatry 93 (2), 169–179. https://doi.org/10.1136/jnnp-2021-326630.

Raffelt, D., Tournier, J.D., Fripp, J., Crozier, S., Connelly, A., Salvado, O., 2011. Symmetric diffeomorphic registration of fibre orientation distributions. Neuroimage. 56 (3), 1171–1180. https://doi.org/10.1016/j.neuroimage.2011.02.014.

Ofori, E., Pasternak, O., Planetta, P.J., Burciu, R., Snyder, A., Febo, M., Golde, T.E., Okun, M.S., Vaillancourt, D.E., 2015. Increased free water in the substantia nigra of Parkinson's disease: a single-site and multi-site study. Neurobiol. Aging 36 (2), 1097–1104.

Archer DB, Coombes SA, Chu WT, et al., A widespread visually-sensitive functional network relates to symptoms in essential tremor, Brain, Feb 1 2018; 141(2), 472-485, 10.1093/brain/awx338.

Archer, D.B., Bricker, J.T., Chu, W.T., et al., Sep 2019. Development and validation of the automated imaging differentiation in parkinsonism (AID-P): a multi-site machine learning study. Lancet Digit Health. 1 (5), e222–e231. https://doi.org/10.1016/s2589-7500(19)30105-0.

Avants, B.B., Epstein, C.L., Grossman, M., Gee, J.C., Feb 2008. Symmetric diffeomorphic image registration with cross-correlation: evaluating automated labeling of elderly and neurodegenerative brain. Med. Image Anal. 12 (1), 26–41. https://doi.org/10.1016/j.media.2007.06.004.

Archer, D.B., Coombes, S.A., McFarland, N.R., DeKosky, S.T., Vaillancourt, D.E., 2019. Development of a transcallosal tractography template and its application to

dementia. Neuroimage. 200, 302–312. https://doi.org/10.1016/j.neuroimage.2019.06.065.
Archer, D.B., Vaillancourt, D.E., Coombes, S.A., 2018. A template and probabilistic atlas of the human sensorimotor tracts using diffusion MRI. Cereb. Cortex 28 (5), 1685–1699. https://doi.org/10.1093/cercor/bhx066.
van Baarsen, K.M., Kleinnijenhuis, M., Jbabdi, S., Sotiropoulos, S.N., Grotenhuis, J.A., van Cappellen van Walsum, A.M., 2016. van Cappellen van Walsum AM. A probabilistic atlas of the cerebellar white matter. Neuroimage. 124, 724–732.
Mak, E., Holland, N., Jones, P.S., Savulich, G., Low, A., Malpetti, M., Kaalund, S.S., Passamonti, L., Rittman, T., Romero-Garcia, R., Manavaki, R., Williams, G.B., Hong, Y.T., Fryer, T.D., Aigbirhio, F.I., O'Brien, J.T., Rowe, J.B., 2021. In vivo coupling of dendritic complexity with presynaptic density in primary tauopathies. Neurobiol. Aging 101, 187–198.
Tsuboi, Y., Slowinski, J., Josephs, K.A., Honer, W.G., Wszolek, Z.K., Dickson, D.W., 2003. Atrophy of superior cerebellar peduncle in progressive supranuclear palsy. Neurology. 60 (11), 1766–1769.
Dutt, S., Binney, R.J., Heuer, H.W., Luong, P., Attygalle, S., Bhatt, P., Marx, G.A., Elofson, J., Tartaglia, M.C., Litvan, I., McGinnis, S.M., Dickerson, B.C., Kornak, J., Waltzman, D., Voltarelli, L., Schuff, N., Rabinovici, G.D., Kramer, J.H., Jack, C.R., Miller, B.L., Rosen, H.J., Boxer, A.L., 2016. Progression of brain atrophy in PSP and CBS over 6 months and 1 year. Neurology. 87 (19), 2016–2025.
Zhang, Y.u., Walter, R., Ng, P., Luong, P.N., Dutt, S., Heuer, H., Rojas-Rodriguez, J.C., Tsai, R., Litvan, I., Dickerson, B.C., Tartaglia, M.C., Rabinovici, G., Miller, B.L., Rosen, H.J., Schuff, N., Boxer, A.L., Yang, S., 2016. Progression of microstructural degeneration in progressive supranuclear palsy and corticobasal syndrome: a longitudinal diffusion tensor imaging study. PLoS ONE 11 (6), e0157218.
Whitwell, J.L., Tosakulwong, N., Schwarz, C.G., Botha, H., Senjem, M.L., Spychalla, A.J., Ahlskog, J.E., Knopman, D.S., Petersen, R.C., Jack, C.R., Lowe, V.J., Josephs, K.A., 2019. MRI outperforms [18F]AV-1451 PET as a longitudinal biomarker in progressive supranuclear palsy. Mov. Disord. 34 (1), 105–113.
Barbagallo, G., Sierra-Peña, M., Nemmi, F., Traon, A.-L., Meissner, W.G., Rascol, O., Péran, P., 2016. Multimodal MRI assessment of nigro-striatal pathway in multiple system atrophy and Parkinson disease. Mov. Disord. 31 (3), 325–334.
Baudrexel, S., Seifried, C., Penndorf, B., Klein, J.C., Middendorp, M., Steinmetz, H., Grünwald, F., Hilker, R., 2014. The value of putaminal diffusion imaging versus 18-fluorodeoxyglucose positron emission tomography for the differential diagnosis of the Parkinson variant of multiple system atrophy. Mov. Disord. 29 (3), 380–387.
Ito, M., Watanabe, H., Kawai, Y., Atsuta, N., Tanaka, F., Naganawa, S., Fukatsu, H., Sobue, G., Jul 2007. Usefulness of combined fractional anisotropy and apparent diffusion coefficient values for detection of involvement in multiple system atrophy. J. Neurol. Neurosurg. Psychiatry 78 (7), 722–728.
Köllensperger, M., Seppi, K., Liener, C., Boesch, S., Heute, D., Mair, K.J., Mueller, J., Sawires, M., Scherfler, C., Schocke, M.F., Donnemiller, E., Virgolini, I., Wenning, G. K., Poewe, W., 2007. Diffusion weighted imaging best discriminates PD from MSA-P: A comparison with tilt table testing and heart MIBG scintigraphy. Mov. Disord. 22 (12), 1771–1776.
Tsukamoto, K., Matsusue, E., Kanasaki, Y., Kakite, S., Fujii, S., Kaminou, T., Ogawa, T., 2012. Significance of apparent diffusion coefficient measurement for the differential diagnosis of multiple system atrophy, progressive supranuclear palsy, and Parkinson's disease: evaluation by 3.0-T MR imaging. Neuroradiology 54 (9), 947–955.
Nicoletti, G., Lodi, R., Condino, F., et al., Oct 2006. Apparent diffusion coefficient measurements of the middle cerebellar peduncle differentiate the Parkinson variant of MSA from Parkinson's disease and progressive supranuclear palsy. Brain. 129 (Pt 10), 2679–2687. https://doi.org/10.1093/brain/awl166.
Sako, W., Murakami, N., Izumi, Y., Kaji, R., 2016. The difference of apparent diffusion coefficient in the middle cerebellar peduncle among parkinsonian syndromes: Evidence from a meta-analysis. J. Neurol. Sci. 363, 90–94. https://doi.org/10.1016/j.jns.2016.02.034.
Braak, H., Del Tredici, K., Rub, U., de Vos, R.A., Jansen Steur, E.N., Braak, E., 2003. Staging of brain pathology related to sporadic Parkinson's disease. Neurobiol. Aging 24 (2), 197–211.
Fearnley, J.M., Lees, A.J., Oct 1991. Ageing and Parkinson's disease: substantia nigra regional selectivity. Brain. 114 (Pt 5), 2283–2301.
Burciu, R.G., Vaillancourt, D.E., Nov 2018. Imaging of motor cortex physiology in parkinson's disease. Mov. Disord. 33 (11), 1688–1699. https://doi.org/10.1002/mds.102.
Mitchell, T., Lehéricy, S., Chiu, S.Y., Strafella, A.P., Stoessl, A.J., Vaillancourt, D.E., 2021. Emerging neuroimaging biomarkers across disease stage in parkinson disease: a review. JAMA Neurol 78 (10), 1262.
Burciu, R.G., Chung, J.W., Shukla, P., Ofori, E., Li, H., McFarland, N.R., Okun, M.S., Vaillancourt, D.E., 2016. Functional MRI of disease progression in Parkinson disease and atypical parkinsonian syndromes. Neurology. 87 (7), 709–717.
Arpin D, Mitchell T, Archer DB, et al., Diffusion MRI detects progression in Parkinson's disease: a placebo-controlled trial of rasagiline, Mov Disord. In Press.
Chary, K., Narvaez, O., Salo, R.A., San Martín Molina, I., Tohka, J., Aggarwal, M., Gröhn, O., Sierra, A., 2021. Microstructural Tissue changes in a rat model of mild traumatic brain injury. Front. Neurosci. 15, 746214 https://doi.org/10.3389/fnins.2021.746214.